Dynamic Tensile Behavior of Materials with Previous Fatigue Damage

U. Sánchez-Santana[a,b], C.Rubio-González[a], G. Mesmacque[b], A. Amrouche[b]

[a] Centro de ingeniería y Desarrollo Industrial, Pie de la cuesta 702, Desarrollo San Pablo, 76130 Querétaro, Qro., México.
[b] Laboratoire de Mécanique de Lille, Université de Lille1, UMR CNRS 8107, Villeneuve d'Ascq 59650, France.

Abstract In different engineering applications such as automobile and train crashes, the high speed impact of debris as well as the high speed manufacturing processes, makes it necessary to have deep understanding of the dynamic behavior of materials and components. There are different experimental techniques to determine the constitutive material behavior and several constitutive models have been proposed to predict the dynamic response of engineering structures. However, in all cases, initial damage free material is assumed and the structures are without fatigue damage when tested. The dynamic response of fatigue damaged steel and aluminum specimens subjected to impact loading is investigated in this work. Samples subjected to previous high cycle fatigue are considered. Results show that previous fatigue damage affects the quasi-static behavior of steel more significantly than that of aluminum. Dynamic yield stress of 6061-T6 aluminum samples is more sensitive to fatigue damage than to strain rate. Previous fatigue damage has a detrimental effect on ductility of 4140T steel, mainly on the dynamic tests.

1 INTRODUCTION

It is well known that the mechanical behavior, such as yield stress, ductility and strength of materials, will change under different strain-rate loadings and temperatures [1]. The consideration of rate dependence on material behavior is very important in the design of structures. An understanding of the deformation of metals over a wide range of temperatures and strain rates is important in metal forming, high speed machining, high velocity impact, penetration mechanics, explosive-metal interaction, and other similar dynamic conditions. Impact problems have been studied for long time. In the numerical simulation for this type of problems, one particular challenge is to characterize the material behavior under high strain-rate loading conditions. A complete material description involves not only stress-strain response as a function of large strains, high strain-rates, high temperatures, stress state and loading history variations, but also the damage accumulation and failure mode [2].

The dynamic behavior of different materials under tensile loading impact has been investigated and reported in the open literature. Tensile impact properties of different magnesium alloys were evaluated in [3] using the split Hopkinson bar. The effect of strain rate on the tensile strength, the elongation at fracture and the absorbed energy was examined. The dynamic response of sheet metals at high strain rates was investigated in [4] with a tensile split Hopkinson bar. After the tensile properties of brass under dynamic loadings based on the tensile impact recovery experiment technique were obtained, [5] a phenomenologically based constitutive model was developed to describe its tensile deformations over a wide range of strain rates. High strain rate tensile testing methods of steel sheets are basic for car body optimization during crash events [6]. A constitutive relation was formulated in [7] to predict changes in specimen geometry and temperature profiles on specimens and it was validated by comparison with experimental results using a tensile Hopkinson bar and high speed photography. In addition, the thermo-mechanical behavior of carbon-epoxy composite materials and polymers has been investigated in [8] and [9], respectively.

Little work has been done to evaluate the effect of previous fatigue damage on the dynamic response of materials and structures. The only work reported [10] considered the effect of pre-damage to the high strain rate behavior, (ignition sensitivity, and impact ignition mechanism) of rocket propellant materials with constant stress and monotonic tension tests performed prior to using the modified Hopkinson bar.

Fatigue damage accumulates and increases with the application of load cycles. Cumulative fatigue damage plays an important role in life prediction of components and structures subjected to field load histories. Since the introduction of the damage accumulation concept, many damage models have been developed [11]. The first damage rule proposed was the Palmgren-Miner model expressed mathematically:

$$D = \sum \left(n_i / N_{fi} \right) \quad (1)$$

where D denotes the damage, and n_i and N_{fi} are the applied cycles and applied cycles to failure under the ith constant-amplitude loading level, respectively. Failure is assumed to occur when D=1. The main deficiencies with linear damage rules (like the Palmgren-Miner model) are the load-level independency and the load-sequence independence.

The aim of this paper is to investigate the effect of previous fatigue damage on the dynamic tensile behavior of samples made of 6061-T6 aluminum alloy and AISI 4140T steel using the split Hopkinson bar apparatus. Different loading rates and previous fatigue damage levels are considered. Quasi-static stress-strain response for different damage levels is evaluated as well. Fatigue damage was introduced on the test specimens by application of cyclic loading under stress control. Next the experimental procedure is described, followed by the results and discussion of them. The influence of previous fatigue damage on quasi-static and dynamic mechanical properties and failure modes on both materials are analyzed. Finally, conclusions are presented.

2 EXPERIMENTAL PROCEDURE

2.1 Test materials and specimen preparation

The structural materials tested were 6061-T6 aluminum alloy and AISI 4140T steel. Al 6061 is Al-Mg-Si-Cu alloy used various applications after T6 heat treatment. AISI 4140T steel is chromium molybdenum alloy steel, oil hardening steel of relatively high hardening ability and is among the most widely used versatile machinery steels. Tables I and II give the chemical composition. The specimen geometry is shown in Figure 1. Chemical composition was determined using a spark emission spectrometer.

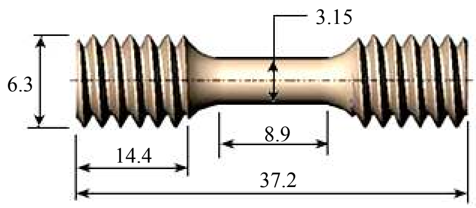

Figure 1. Specimen used in the quasi-static, fatigue and dynamic tests. Dimensions in mm

Table I. Chemical composition of 6061-T6 aluminum alloy (wt. percent).

Material	Si	Fe	Mg	Zn	Cu	Mn	Cr	Ti
6061-T6 aluminum alloy	.52	.27	.46	.01	.13	.03	.027	.02

Table II. Chemical composition of AISI 4140 steel (wt. percent).

Material	C	Mn	Si	Cr	Mo	P	S
AISI 4140T steel	.38	.75	.20	.80	.15	.40	.04

2.2 Fatigue tests

Stress controlled fatigue tests performed on an INSTRON8501 servo hydraulic machine allowed the determination of *S-N* curves applying uniaxial cyclic loading between constant stress limits with stress ratio $R=\sigma_{min} / \sigma_{max}$ =0.2. The smooth specimens used had 3.15mm in diameter at center, see Figure 1. Cyclic loading with sinusoidal wave form at frequency of 35Hz was applied. Knowing the fatigue life (the complete *S-N* curve was determined for each material), it was possible to induce fatigue damage on the tensile specimens at damage levels of D=0.25, 0.50 and 0.75 (see equation (1)). To determine the fatigue life, N_{fi}, of 6061-T6 aluminum alloy, constant amplitude cyclic loading was applied on the specimens between σ_{min}=56MPa and σ_{max}=282MPa, that is, the stress ratio was R=0.2. Fatigue life determined under this loading condition was N_{fi}=430,000 cycles. For AISI 4140T steel specimens, the cyclic loading between σ_{min}=146MPa and σ_{max}=731MPa developed a fatigue life of N_{fi}=447,000 cycles. For example, steel specimens were subjected to 111,750 cycles of loading between σ_{min}=146MPa and σ_{max}=731MPa to generate a fatigue damage D=0.25. Fatigue damage has been estimated using the Palmgren-Miner rule.

2.3 Impact test apparatus and dynamic tests

The Hopkinson bar test has been widely accepted to produce strain rates in the order of 10^2 to 10^4 s^{-1}. The apparatus consists mainly of an air gun, a projectile, two Hopkinson pressure bars (one incident and one transmitter), a velocity measuring device and recording equipment, see Figure 2. The two elastic bars are long and slender steel bars of high resistance. The incident bar (2470mm long) and the transmitter bar (1050mm long) were made of 19mm diameter high strength steel (Maraging C300).

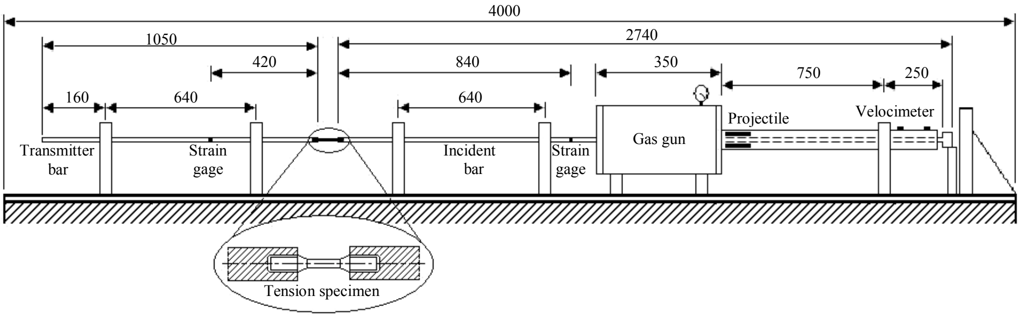

Figure 2. Schematic illustration of the tension Hopkinson bar. Dimensions in mm.

The striker tube or projectile (outer diameter 31.8mm, inner diameter 19.15mm and length 105mm) was made of the same steel. The specimen was placed between the incident and the transmitter bars using threaded ends (1/4" -20UNC). The striker tube is fired from the air gun and impacts an anvil. From the impact, a tensile pulse is generated in the incident bar and propagates into the specimen. Part of the incident pulse is transmitted into the specimen and propagates through the transmitter bar. The rest of the pulse reflects into the incident bar as a compressive pulse. The impact produces tensile waves propagating with speed C_0 along the projectile and the incident bar, where $C_0 = (E/\rho)^{1/2}$, being E the elastic modulus and ρ the bar material density. The transmitted and reflected pulses are measured using strain gages (VISHAY CEA-06-062-UW-120) one attached to each bar using M Bond 200 adhesive. The first strain gage was located 840mm from the impact end of the incident bar (close to the specimen); and the other strain gage was placed 420mm from the end of the transmitter bar (close to the specimen), see Figure 2. The output signals of the strain gages were conditioned by conditioners VISHAY 2311 and then visualized and stored into an oscilloscope Agilent model Infiniium 5483 where the signals were recorded at a sampling rate of 1μs. Figure 3 represents incident, reflected and transmitted pulses recorded on a typical experiment.

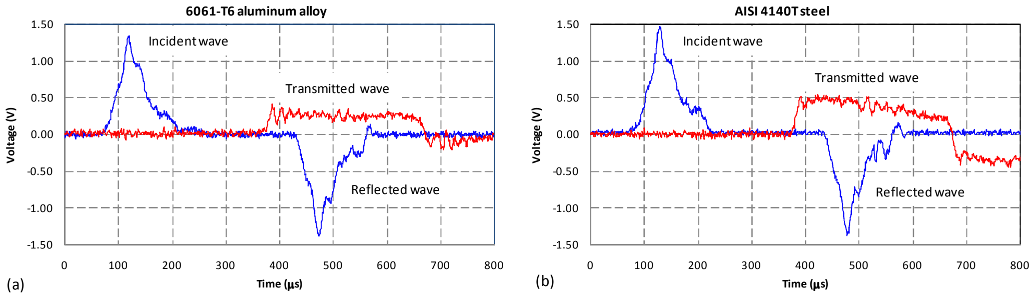

Figure 3. Typical pulses acquired on the dynamic tension tests of specimens for stress controlled fatigue. (a) For 6061-T6 aluminum alloy, (b) for AISI 4140T steel.

Measuring the amplitude of the incident, reflected and the transmitted pulses, ε_I, ε_R and ε_T respectively, as those shown in Figure 3, it is possible to determine the stress-strain relationship of the specimen. It is possible to show [12, 13] that the strain rate $d\varepsilon(t)/dt$ (a function of time) is calculated as

$$\dot{\varepsilon} = \frac{d\varepsilon}{dt} = \frac{2C_0}{L}\varepsilon_R \tag{2}$$

where L_s is the effective length of the specimen. The strain is found by integrating the strain rate from 0 to t

$$\varepsilon(t) = \left(\frac{2C_0}{L}\right)\int_0^t \varepsilon_R dt \tag{3}$$

By force equilibrium at bar interface, the following equation for the stress as a function of time acting on the specimen may be developed

$$\sigma(t) = E\left(\frac{A_0}{A}\right)\varepsilon_T(t) \tag{4}$$

where A_0 is the cross sectional area of the incident bar and A the cross sectional area of the specimen. Three fatigue damage levels were considered: D=0.25, 0.50 and 0.75; and three projectile speeds were used on the Hopkinson bar tests v=18m/s, 25m/s and 30m/s.

3 RESULTS AND DISCUSSION

3.1 Fatigue Tests

Even though fatigue life was needed only at a given stress conditions, the complete S-N curves were determined for both materials: 6061-T6 aluminum alloy and AISI 4140T steel (Figure 4). Fatigue life, N_f, may be determined from those curves for a given maximum stress σ_{max} (MPA) with stress ratio R =0.2. Fitting the experimental results, the S-N curves may be described by the following Basquin type equations:

$$\sigma_{max} = 1158.4 N_f^{-0.1095}$$ for 6061-T6 aluminum alloy

$$\sigma_{max} = 1166.1 N_f^{-0.036}$$ for AISI 4140T steel

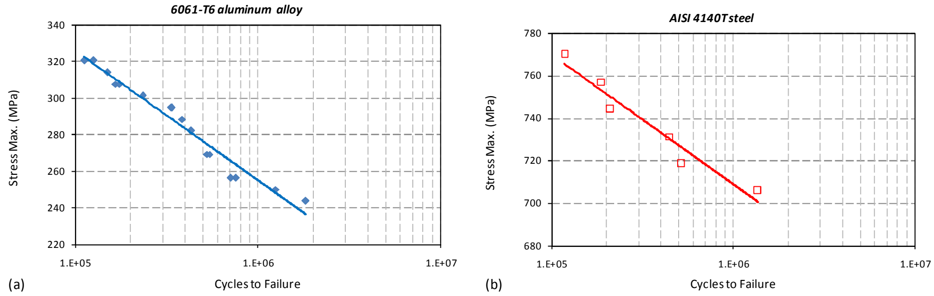

Figure 4. S-N curves of 6061-T6 aluminum alloy (a) and AISI 4140T steel (b). In both cases R=0.2.

3.2 Quasi-static tension tests

To determine the influence of previous fatigue damage, quasi-static tension tests were performed on specimens with fatigue damage D=0.25, 0.50, and 0.75. Quasi-static stress-strain curves for each material were determined and are shown in Figure 5 with stress-strain curves of damage-free materials included for comparison. Table III gives the mechanical properties at room temperature of damage free material. Quasi-static mechanical properties of both materials were obtained on a MTS810 machine applying monotonic load at constant speed of 3mm/min for aluminum and 1 mm/min for steel.

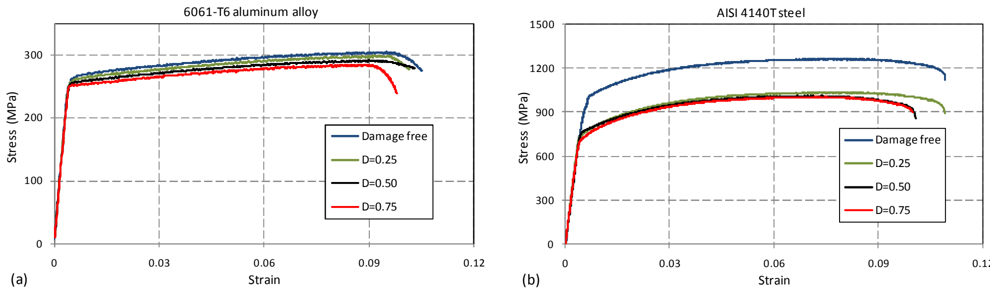

Figure 5. Quasi-static stress-strain curves of (a) 6061-T6 aluminum alloy and (b) AISI 4140T steel for different damage levels.

From those results it is possible to observe that there is no significant effect of previous fatigue damage on the stress-strain response of Al6061-T6. Young's modulus is approximately the same, the yield stress decreases slightly as the damage level increases and the ultimate stress exhibits the same behavior. On the other hand, note that the stress-strain response of steel 4140T is affected by the previous fatigue damage. The Young's modulus is approximately the same with and without fatigue damage; however, the yield stress is significantly higher for the damage-free material and does not change significantly with the damage level after D=0.25. The same behavior is observed for ultimate stress. For a summary of the quasi-static mechanical properties see Table III; the yield strength reported in Table III was obtained employing the 0.2% offset method. Young's modulus, yield stress and ultimate stress of 6061-T6 aluminum alloy and AISI 4140T steel are shown for different damage levels.

Table III. Quasi-static mechanical properties at different damage levels.

	6061-T6 Aluminum Alloy				AISI 4140T Steel			
	Damage free	0.25	0.50	0.75	Damage free	0.25	0.50	0.75
Young´s modulus (GPa)	65	65	65	65	183	183	183	183
Yield stress (MPa)	264	260	256	251	1026	778	789	748
Ultimate stress (MPa)	304	299	291	284	1265	1037	1014	1005

3.3 Dynamic tension tests

Dynamic stress-strain curves obtained by using the Hopkinson bar apparatus and equations (2) and (3) for 6061-T6 aluminum alloy and AISI 4140T steel are shown in Figures 6. Quasi-static stress-strain curves for damage free materials are included for comparison.

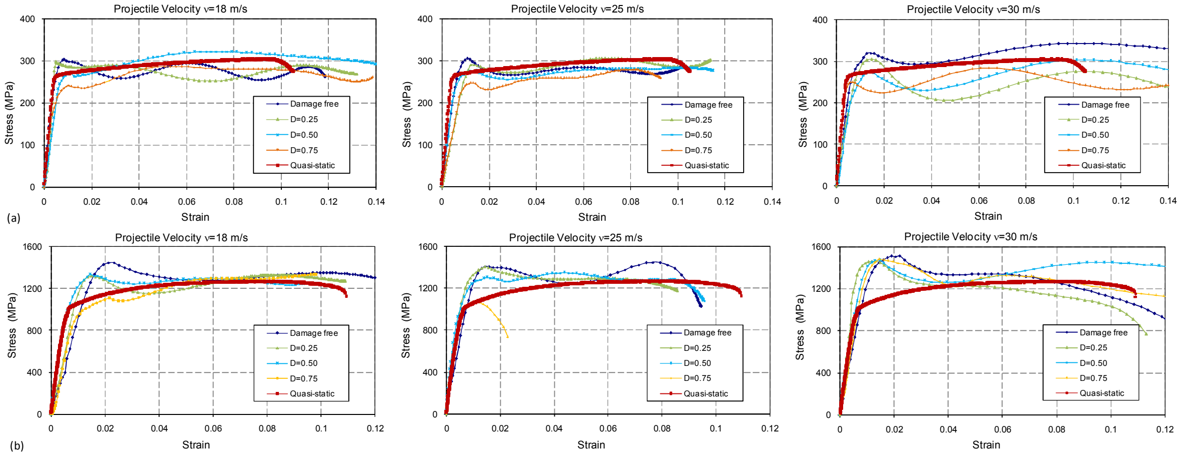

Figure 6. Dynamic stress-strain curves for (a) 6061-T6 aluminum alloy and (b)AISI 4140T steel at different strain rates and damage levels.

Different damage levels and projectile velocities (strain rates) were considered. Note that in all cases the yield stress decreases as the damage level increases. This effect is better appreciated on Figure 7 where the influence of strain rate is presented as well.

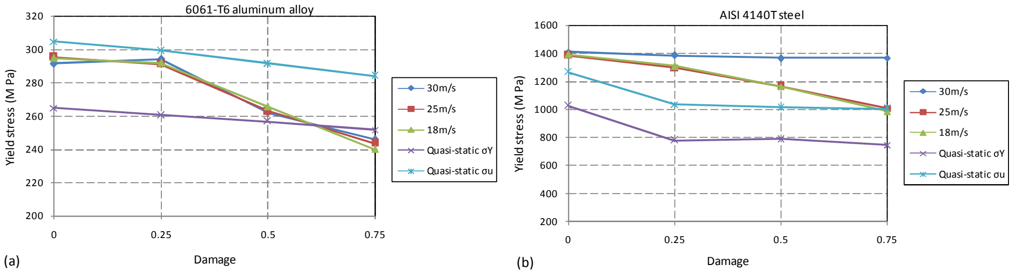

Figure 7. Effect of fatigue damage on quasi-static and dynamic mechanical properties of (a) 6061-T6 aluminum alloy and (b) AISI 4140T steel.

Analyzing the effect of fatigue damage on the quasi-static behavior of 6061-T6 aluminum alloy shown in figure 7(a), we observe that there is a small decrease of about 5% in the yield stress, σ_y, and about 6% in the ultimate stress, σ_u, when increasing the damage level, D. The stability of quasi-static mechanical properties at different damage levels enhances the behavior of this structural aluminum alloy. The steel response is different. Observe in Figure 7(b) that σ_y decreases about 27% and σ_u about 20% increasing the damage level, that decrease is more important at low damage levels, there is a big change on the mechanical properties from D=0 to D=0.25. After D=0.25 σ_y and σ_u remain almost stable. We conclude that previous fatigue damage affects more significantly the quasi-static mechanical properties of steel than aluminum.

The effect of fatigue damage on the dynamic yield strength is also shown on Figure 7. Figure 7(a) shows the influence on aluminum. There is a reduction on σ_y of about 18% increasing D. That reduction is more important after D=0.25. Note that σ_y is not affected appreciably by the strain rate or the projectile velocity v, it changes only when the damage level is varied. Looking at Figure 7(b), the steel case, it is observed that the yield stress is not affected by the damage level at high strain rates (projectile velocity v=30m/s), σ_y is almost constant at different values of D. However, at low strain rates (v=18m/s) the influence of D on σ_y is important; there is a reduction of about 29% on σ_y when increasing the damage level. That reduction occurs at an approximately constant rate when increasing D.

3.4 Effect on ductility

To assess the effect of previous fatigue damage and strain rate on ductility of the aluminum and steel samples, two ductility related parameters were evaluated: the percent elongation, $\%\varepsilon_f$, and the percent reduction in area, $\%RA$, given by [14]

$$\%\varepsilon_f = 100\frac{L_f - L_i}{L_i} \qquad \%RA = 100\frac{A_i - A_f}{A_i}$$

these parameters compare the gage section final length, L_f, with the initial L_i; and the cross-sectional area after fracture, A_f, with the original area A_i.

Figure 8 shows the $\%\varepsilon_f$ and the $\%RA$ for different damage levels and projectile speeds of 6061-T6 aluminum samples. Note in Figure 8(a) that $\%\varepsilon_f$ increases (approximately from 35% to 40%) increasing the damage level, but it is not affected by the strain rate. The evolution of the quasi-static $\%\varepsilon_f$ with damage is included as well and it changes from 5% to 8% when D goes from 0 to 0.75. The percent reduction in area is not affected by the strain rate either, as shown in Figure 8(b), but it changes (from approximately 32% to 38%) increasing the damage level; while the quasi-static $\%RA$ changes from 27% to 31%. Thus, fatigue damage slightly enhances the ductility of 6061-T6 aluminum samples in quasi-static and dynamic tension tests.

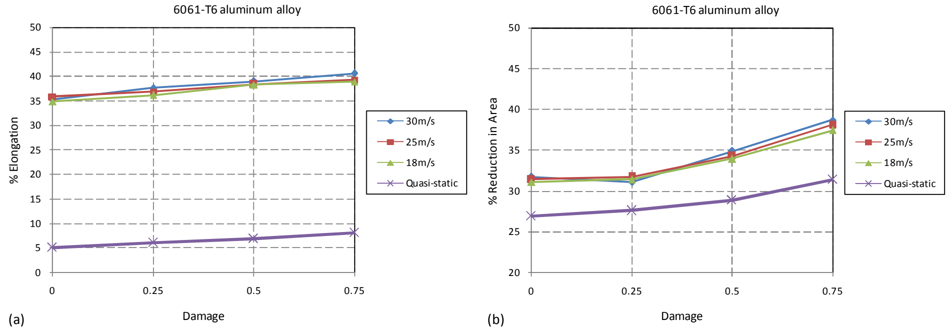

Figure 8. Effect of fatigue damage on ductility parameters of 6061-T6 aluminum alloy (a) percent elongation and (b) percent reduction in area.

The percent elongation and the percent reduction in area of steel specimens are shown in Figure 9. Note in Figure 9(a) that $\%\varepsilon_f$ decreases considerably on the dynamic tests as D increases. This loss of ductility is more important after D=0.5. There is a decrease of about 32% when increasing damage from D=0 to 0.75. Also, there is a small effect of the projectile speed on this parameter. From the results of the quasi-static tests, $\%\varepsilon_f$ does not change when increasing D. A similar behavior is observed for $\%RA$ shown in Figure 9(b). On the dynamic response there is a loss of about 18% when increasing damage from D=0.75 to 0 and the projectile speed shows only slight effects. For the quasi-static tests $\%RA$ changes from 8% to 3% increasing D. Hence, previous fatigue damage has a detrimental effect on ductility of 4140T steel, mainly on the dynamic tests.

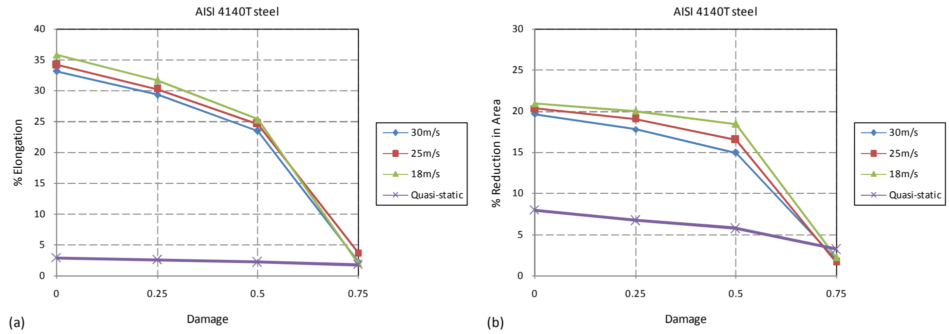

Figure 9. Effect of fatigue damage on ductility parameters of AISI 4140T steel (a) percent elongation and (b) percent reduction in area.

3.5 Failure modes

Figures 10(a) and 10(b) show the effect of fatigue damage and strain rate on the failure modes of aluminum and steel samples on the dynamic experiments. Note that for the aluminum case, the fracture surface is approximately normal to the specimen axis regardless the damage level D and the strain rate (projectile velocity). In addition, note that significant necking is appreciated in all the cases. In Figure 10(b) observe that the effect of D on the behavior of steel is different from that shown on aluminum. The fracture surface plane is oriented about 45^o with respect to the specimen axis when v=18m/s and approximately 60^o when v=25m/s for damage free materials, while that angle is near 90^o when D=0.75 for both projectile speeds. In other words, yielding occurs on specimens with small values of D presenting fracture surfaces at inclined planes, while fracture surfaces become normal at high values of D.

a)

Aluminum v=18m/s

Aluminum v=25m/s

Aluminum v=30m/s

(b)

Steel v=18m/s

Steel v=25m/s

Steel v=30m/s

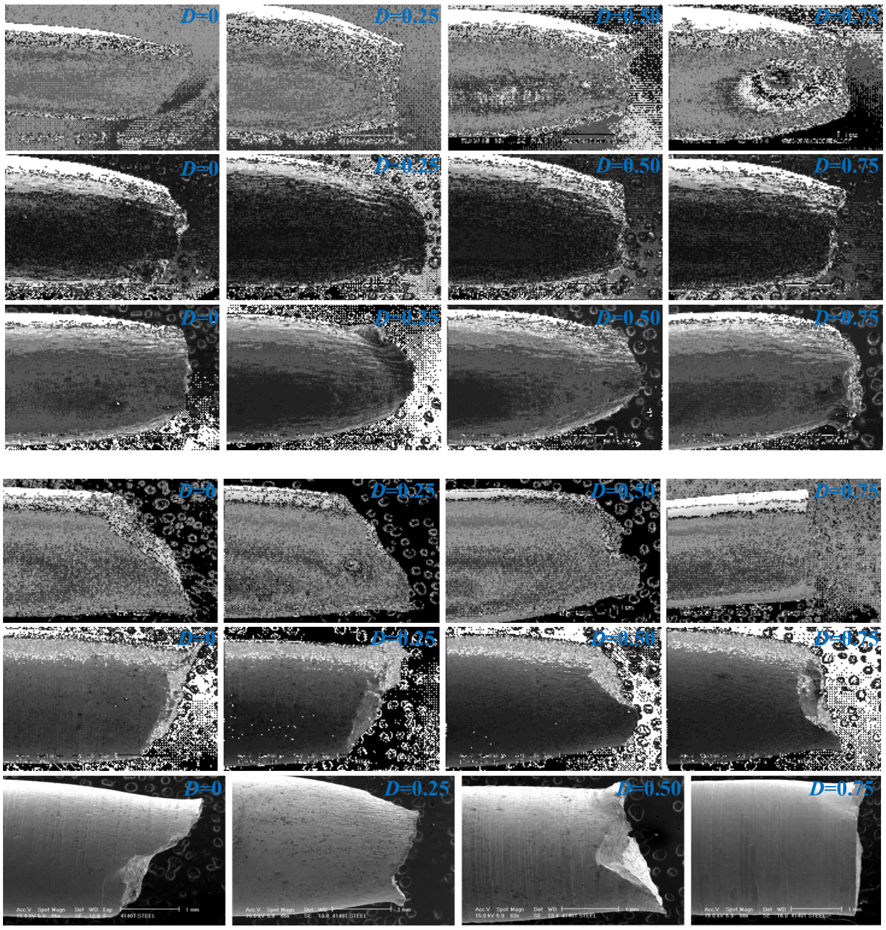

Figure 10. Fracture modes of (a) 6061-T6 aluminum alloy and (b) AISI 4140T steel at different strain rates and fatigue damages.

This suggests a transition on the steel behavior increasing *D*; a ductile response is observed at small values of *D* while a brittle behavior is exhibited by the material at high damage levels.

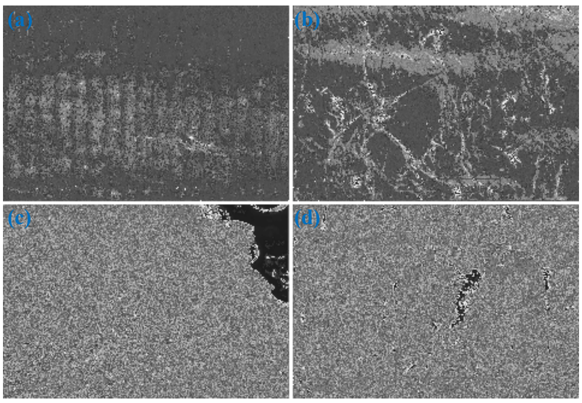

Figure 11. Micro-photographs of the specimen surface without and with previous fatigue damage after the quasi-static tension test. (a) aluminum with no damage, (b) aluminum with D=0.75, (c) steel with no damage, (d) steel with D=0.25.

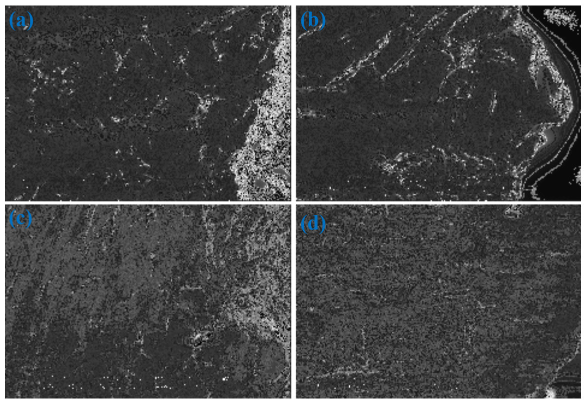

Figure 12. Micro-photographs of the specimen surface without and with previous fatigue damage after the dynamic tension test, in all cases the projectile speed was v=30m/s. (a) aluminum with no damage, (b) aluminum with D=0.25, (c) steel with no damage, (d) steel with D=0.25.

A closer view of images presented in Figure 10 is shown in Figures 11 and 12. Figure 11 presents the specimen surface after the quasi-static tension test. Note that specimens without damage exhibit a clean surface after the tension test, while specimens with previous fatigue damage present slip steps (specially aluminum Figure 11(b)) and surface cracks (mainly for steel Figure 12(d)). Similarly, Figure 12 shows the specimen surface close to the fracture zone after the dynamic tension tests. Note severe surface damage on aluminum specimens, Figure 12(a) and 12(b), slip bands oriented approximately 45^{o} from the specimen axis are observed.

4 CONCLUSIONS

The influence of previous fatigue damage on the quasi-static and dynamic tensile behavior of 6061-T6 aluminum alloy and AISI 4140T steel has been evaluated. Dynamic tension tests were performed on a Hopkinson bar apparatus.

From the quasi-static tension tests of aluminum, a small decrease on the yielding stress (around 5%) and ultimate stress (around 6%) result when increasing the damage level. The stability of quasi-static mechanical properties at different damage levels enhances the behavior of this structural aluminum alloy. On the other hand, the steel exhibited a different response. The yield and ultimate stresses are significantly higher for the damage-free material and do not change significantly with the damage level, they remain almost constant after D=0.25.

The dynamic response of aluminum shows a reduction in the yield stress of about 18% as *D* increases. The yield stress is not affected significantly by the strain rate or the projectile velocity, *v*. For steel, the yield stress is not affected by the damage level at high strain rates; however, at low strain rates the influence of damage on the yield stress is important, it decreases about 40% when increasing the damage level.

From the failure surface analysis of the aluminum samples, the fracture surface was approximately normal to the specimen axis regardless the damage level or the strain rate (projectile velocity); in addition, a significant necking was appreciated in all the cases. Ductility of aluminum is slightly enhanced when increasing *D* on the quasi-static and dynamic tests. Severe surface damage on aluminum specimens was observed after the dynamic tension tests.

The behavior of steel was different, fracture surface plane was oriented about 45^o to 60^o with respect to the specimen axis for damage-free specimens, while that angle was near 90^o when *D*=0.75 for all projectile speeds. In other words, yielding occurs on specimens with small values of *D* presenting fracture surfaces at inclined planes, while fracture surfaces become normal at high values of *D*. This suggests a transition on the steel behavior increasing *D*; a ductile response is observed at small values of *D* while a brittle behavior is exhibited by the material at high damage levels. This is in agreement with the decrease in $\%\varepsilon_f$ and %*RA* when the damage level is increased.

5 REFERENCES:

[1]. M. A. Meyers, Dynamic Behavior of Materials, Wiley Interscience Publication, 1994.
[2]. J. A. Zucas, Impact Dynamics, Wiley. 1990.
[3]. T. Yokoyama, *Strain* 39(2003)167-175.
[4]. H. Huh, W. J. Kang and S.S. Han, *Experimental Mechanics*, 42 (2002) 8-17.
[5]. Y. Wang, Y. Zhou and Y. Xia, *Materials Science and Engineering A*, 372(2004) 186-190.
[6]. A. Uenishi, Y. Kuriyama, H. Yoshida and M. Takahashi, *Nippon Steel Technical Report*, 88 (2003) 22-26.
[7]. J.P. Noble, B.D. Goldthorpe, P. Church, J. Harding, *Journal of the Mechanics and Physics of Solids 47* (1999) 1187-1206.
[8]. Z. Li, J. Lambros, *Composites A 31*(2000) 537-547.
[9]. W. Chen, F. Lu, M. Cheng, *Polymer Testing 21* (2002) 113-121.
[10]. S. Y. Ho, *Combustion and Flame* 1996;104:524-534.
[11]. A. Fatemi, L. Yang, *Int. J. Fatigue* 1998;20:9-34
[12]. H. Kolsky, *Stress waves in solid media*, Dover Publications, 1963.
[13]. K. F. Graff, *Wave motion in elastic solids*. Dover Publications 1991.
[14]. N.E. Dowling, Mechanical Behavior of Materials, Prentice Hall 2007.